Journal of Engineering and Technology for Industrial Applications

ISSN ONLINE: 2447-0228

ITEGAM-JETIA

Manaus, v.11 n.55, p. 276-292. September/October, 2025.

DOI: https://doi.org/10.5935/jetia. v.11 n.55.2713

RESEARCH ARTICLE OPEN ACCESS

COMBINED EFFECT OF GLASS POWDER AND RECYCLED SAND ON FRESH AND HARDENED PROPERTIES OF STEEL FIBER-REINFORCED SELF-COMPACTING CONCRETE

Souhila Fergani[1], Said Zaouai[2], Rachid Rabehi[3] and Ali Abbache[4]

[1, 3, 4] Faculty of Civil Engineering, University of Science and Technology Houari Boumediene (USTHB), Bab Ezzouar, 16111 Algiers, Algeria.
[2] Laboratory of Eco-Materials: Innovations & Applications (EMIA), Civil Engineering Department, University of Djelfa, 17000, Algeria.

[1]https://orcid.org/0009-0005-7086-8141, [2]https://orcid.org/0009-0009-5936-1074
[3]https://orcid.org/0000-0002-9398-7291, [4]https://orcid.org/0009-0002-6257-4336

Email: sfergani@usthb.dz, said.zaouai@univ-djelfa.dz, rachid.rabehi@usthb.edu.dz, ali.abbache@usthb.edu.dz

ARTICLE INFO

Article History
Received: September 19, 2025
Revised: October 3, 2025
Accepted: October 8, 2025
Published: October 31, 2025

Keywords:
Self-compacting concrete,
Waste glass powder,
Recycled sand,
Steel fibers,
Response surface methodology.

ABSTRACT

This study investigates the synergistic effects of waste glass powder and recycled sand on steel fiber-reinforced self-compacting concrete through systematic mixture optimization. Waste glass powder (WGP) and recycled sand (RS) from construction demolition waste were evaluated as sustainable replacements for cement and natural aggregates. The experimental program examined WGP replacement levels of 5-20%, RS substitution of 15-60%, and hooked-end steel fiber incorporation at 0.3-1.2% by volume, maintaining water-to-binder ratio of 0.42 with optimized superplasticizer dosage. Fresh properties were assessed through standardized workability tests including slump flow, V-funnel, and L-box evaluations, while hardened performance encompassed compressive and flexural strength development alongside durability parameters. Design-Expert 13 software facilitated response surface methodology optimization, revealing complex material interactions that challenge conventional additive assumptions. The optimal sustainable formulation comprising 15% waste glass powder, 15% recycled sand, and 0.9% steel fibers achieved balanced performance characteristics. This mixture demonstrated compressive strengths of 53.4 MPa at 28 days, progressing to 64.8 MPa at 90 days, enhanced flexural capacity of 8.2 MPa, and reduced water absorption from 4.2% to 3.8%. Fresh properties remained within acceptable self-compacting concrete criteria despite substantial waste material incorporation. The research demonstrates that waste-derived materials enhance concrete performance when integrated through systematic design approaches, advancing sustainable construction technologies.

I. INTRODUCTION

Concrete has served as the backbone of construction since its earliest use in ancient civilizations, where it enabled the development of durable and enduring structures. Over the centuries, it has evolved into one of the most essential building materials worldwide, underpinning advancements in infrastructure and architectural design. Its significance lies in a rare combination of properties: high compressive strength, adaptability to diverse applications, and cost-effectiveness. Capable of being molded into almost any form while ensuring long-term durability, concrete remains indispensable across all sectors of construction and public works—from monumental dams and extensive highway networks to bridges, tunnels, and modern high-rise buildings.

The foundational development of Portland cement during the 19th century marked a turning point, granting concrete unprecedented consistency and strength. Since then, global concrete production has soared, now exceeding 10 billion tonnes annually. This pervasive use, while instrumental in economic growth and societal development, comes with critical environmental consequences. Cement manufacturing alone contributes around 7–8% of global anthropogenic CO_2 emissions [1], stemming from both the energy-intensive firing

process and chemical decarbonation of limestone. If current trajectories continue, global concrete demands are projected to approach 20 billion m³ by 2050, potentially doubling the associated carbon footprint unless mitigated [2]. In addition to emissions, material consumption poses sustainability challenges. The relentless extraction of natural sand and gravel for concrete depletes riverbeds and coastal areas, threatening ecosystems and undermining resource availability for future generations [3]. Despite this, no material currently matches concrete's aggregate performance, resilience, or cost-effectiveness for large-scale infrastructure. Thus, the pathway forward is not to replace concrete, but to reimagine it—making it greener and more circular [4].

Self-compacting concrete (SCC) represents such an evolution. Pioneered in Japan in the late 1980s, SCC flows under its own weight into formworks, even in fully reinforced zones, eliminating the need for vibration. This innovation streamlines construction, improves surface finish, enhances safety, and increases productivity [5]. However, SCC typically requires high binder content and chemical admixtures, diminishing its potential sustainability benefits and imposing economic constraints [6]. To address these limitations, the research community has turned toward sustainable supplementary materials and recycled aggregates that can partially replace key constituents of SCC [7], [8]. Among these recycled materials are those that replace coarse and/or fine aggregates with various other materials to improve or maintain their physical mechanical properties. These include plastic aggregates, recycled concrete aggregates, and rubber aggregates. Other materials that replace cement are limestone powder, pozzolans, silica fume, ground sand, metakaolin, and glass powder.

Waste glass powder (WGP) is increasingly recognized as an effective supplementary cementitious material (SCM). When finely ground (typically <75 μm), glass powder reacts pozzolanically with calcium hydroxide to form additional calcium silicate hydrate (C–S–H), thus enhancing matrix density and durability while mitigating alkali-silica reaction risks common in coarser glass additions [9–11]. For glass powder with a diameter of less than 75 μm the pozzolanic reaction is largely privileged over ASR [12]. WGP inclusion (10–30% replacement) has demonstrated reductions in permeability, shrinkage, and chloride ingress, with many studies confirming that SCC's fresh and hardened properties remain satisfactory or even improved [13], [14].

On the other hand, the use of recycled sand from construction and demolition waste offers a sustainable alternative to depleting natural sand reserves. Although recycled sand has higher water absorption and angularity, judicious mix design can enable up to 50% replacement without compromising SCC's performance [15]. Such substitutions also support local resource reuse, reducing both material transport impacts and landfill burdens [16]. Additionally, studies have shown that recycled aggregates can be successfully used in percentages of up to 50 wt.% with water absorption values below 6.0% [17].

Despite these two areas receiving attention separately, few studies have pursued a combined assessment of WGP, recycled sand, and steel fiber reinforcement in SCC. The inclusion of steel fibers further addresses concrete's brittleness, enhancing flexural toughness, post-cracking ductility, and impact resistance. For instance, even at low volume fractions, fibers significantly influence mechanical behavior and durability, though they can reduce fresh workability if not properly dosed [18], [19].

While binary combinations—such as WGP with fibers or recycled materials with fibers—have been explored, the simultaneous integration of all three sustainable constituents in SCC remains largely underinvestigated. Recent studies have demonstrated that the combined use of recycled aggregates and waste glass powder can enhance both mechanical performance and durability while contributing to resource efficiency [20]. Similarly, research on fiber-reinforced SCC highlights the need for mixture designs that comply with EFNARC criteria to maintain adequate workability while achieving improved toughness and ductility [21]. These findings underscore the necessity of a holistic approach that considers the coupled effects of WGP, RS, and SF to develop optimized, sustainable SCC mixtures for structural and infrastructure applications.

Moreover, real-world deployment necessitates evidence of practicality. SCC formulations that leverage locally available recycled materials could drastically reduce embodied carbon, transportation emissions, and waste management costs while bolstering structural resilience. Such approaches align with circular economy goals and regulatory pushes for low-carbon construction [22], with recent life cycle assessment studies revealing that incorporating recycled supplementary cementitious materials as cement substitutes can achieve substantial embodied carbon reductions—up to 56% for ground granulated blast-furnace slag, 21% for calcined marine clay, and 16% for waste glass powder—while maintaining structural performance [23].

This This study addresses a key research gap by evaluating self-compacting concrete incorporating waste glass powder as a partial cement replacement, recycled sand as fine aggregate, and steel fiber reinforcement. The work investigates fresh properties (flowability, passing ability, segregation resistance), mechanical performance (compressive and flexural strength), and durability through water absorption tests. Synergistic interactions among these constituents were analyzed using response surface methodology to optimize mixture proportions that preserve self-compacting behavior while enhancing mechanical response. The findings provide a practical framework for implementing waste-derived materials in SCC without compromising structural integrity.

II. MATERIALS AND METHODS

II.1 MATERIALS

II.1.1 Cement

Portland cement conforming to CPA CEM I/52.5 specification was employed throughout this study. The chemical composition, mineralogical characteristics, and physical properties of the cement are presented in Tables 1, 2, and 3, respectively. The specific surface area was determined using the Blaine method, while chemical analysis was conducted through X-ray fluorescence spectroscopy (XRF). Mineralogical composition was calculated using Bogue's equations based on the chemical analysis results [24].

Table 1: Chemical composition of cement used (%).

SiO_2	CaO	Al_2O_3	Fe_2O_3	SO_3	MgO	K_2O	SO_3	Na_2O	LOI
20,87	62,36	5,1	3,42	2,92	1,88	0,68	2,92	0,11	1,8

Source: Authors, (2025).

Table 2: Mineralogical composition of cement used (%).

Mineralogical composition (%)			
C_3S	**C_3A**	**C_2S**	**C_4AF**
62,36	07,06	14,85	12,14

Source: Authors, (2025).

Table 3: Physical properties of cement used.

Properties	**CEM I/B**
Specific density (kg/m^3)	3096
Apparent density (kg/m^3)	1026
Fineness (cm^2/g)	3912
Initial setting time (min)	185
Final setting time (min)	245

Source: Authors, (2025).

II.1.2 Sand

Natural alluvial sand with particle size distribution of 0/5 mm was used as fine aggregate. The sand was sourced from the Oued M'zi region, located north of Laghouat city (Algeria). Prior to use, the sand was washed and dried to remove organic impurities and ensure consistent moisture content. The sand exhibited a fineness modulus of 2.28, classifying it as medium sand according to established grading standards. Physical properties including specific gravity, water absorption, and particle size distribution were determined in accordance with relevant ASTM standards. Table 4 shows the properties of the natural sand used, and Figure 1 presents its visual appearance.

Figure 1: Natural alluvial sand (0–5 mm) used as reference fine aggregate.
Source: Authors, (2025).

Recycled sand was produced through controlled crushing and processing of construction and demolition waste concrete. The source concrete specimens, measuring 0.40 × 0.40 × 0.15 m³, were initially prepared with a cement content of 400 kg/m³ using natural alluvial sand and quartz-based aggregates. After a standard 28-day water-curing period, the hardened concrete was mechanically crushed using a jaw crusher, followed by secondary impact crushing to achieve the desired particle size distribution. The crushed material was subjected to systematic screening to separate the recycled sand fractions with a 0–5 mm particle size distribution, comparable to that of the reference natural sand in accordance with ASTM C33 [25] and EN 12620 [26]. Due to its higher water absorption capacity and modified surface texture compared to natural sand, the recycled sand required careful mix design adjustments to maintain the workability of the self-compacting concrete matrix. Physical and mechanical properties of recycled sand were determined according to standard procedures: specific gravity and water absorption following ASTM C128 [27] (equivalent to EN 1097-6) [28]; fineness modulus by sieve analysis according to ASTM C136 [29] (equivalent to EN 933-1) [30]; and bulk density (apparent volume mass) in accordance with ASTM C29 [31] (equivalent to EN 1097-3) [32]. The results are presented in Table 4, and Figure 2 shows the recycled sand obtained from this process.

Figure 2: Recycled sand (0–5 mm) produced from processed construction and demolition waste concrete.
Source: Authors, (2025).

II.1.3 Gravel

The coarse aggregate used in this study was crushed limestone gravel sourced from the "Zaccar" quarry, south of Djelfa. Two size fractions, 3/8 mm and 8/16 mm, were utilized. As presented in Table 4, both fractions exhibited similar absolute densities (2.66 g/cm³) and low water absorption values (2.3% and 2.2%), indicating limited porosity and good dimensional stability. The Los Angeles abrasion coefficients (25.3% and 25.1%) confirm adequate mechanical resistance. The angular morphology of the particles, resulting from the crushing process, is expected to improve aggregate interlocking and enhance the mechanical performance of the concrete.

Table 4: Physical-mechanical properties of gravel and different types of sand.

Property	**Sand**		**Gravel**	
	Natural	**Recycled**	**Natural**	
	$(0/5)_N$	$(0/5)_R$	$(3/8)_N$	$(8/16)_N$
Apparent volume mass (g/cm^3)	1.52	1.22	1.34	1.39
Absolute density mass (g/cm^3)	2.63	2.49	2.66	2.66
Degree of absorption (%)	1.14	7.7	2.3	2.2
Fineness modulus	2.29	2.23	–	–
Sand equivalent (%)	87.9	–	–	–
Coefficient Los Angeles (%)	–	–	25.3	25.1

Source: Authors, (2025).

II.1.4 Steel Fibers (SF)

MEDAFAC steel fibers with undulated geometry were incorporated into the self-compacting concrete mixtures to enhance mechanical performance and post-cracking behavior. The fibers feature a wavy configuration along their length, providing enhanced mechanical anchorage within the concrete matrix compared to straight fibers.

The physical and geometric properties of the MEDAFAC steel fibers are presented in Table 5. The fibers have a length of 50 mm, width of 2 mm, and density of 7.6 g/cm³. The undulated geometry improves bond characteristics and load transfer capacity through enhanced mechanical interlocking with the surrounding cement matrix.

Table 5: Physical properties of MEDAFAC steel fibers.

Property		**Figure 3 :** Steel fiber used
Absolute density (g /cm^3)	7.60	
Tensile strength	1200 MPa	
Geometry of steel fiber used	D_f = 2 mm L_f = 50 mm Undulated	
Aspect ratio (L_f/D_f)	25	

Source: Authors, (2025).

II.1.5 Mixing Water

Potable tap water meeting drinking water standards was used for all concrete mixtures. The water was maintained at a temperature of 20 ± 1°C during mixing operations to ensure consistent hydration kinetics and workability characteristics across all experimental batches.

II.1.6 Superplasticizer

A third-generation superplasticizer based on polycarboxylate ether technology (MEDAPLAST SP 40) was employed to achieve the required flow characteristics for self-compacting concrete. The admixture exhibited the following properties: pH of 8.2, specific gravity of 1.20 ± 0.01, chloride ion content of <1 g/L, and solid content of 40%. The superplasticizer dosage was optimized through fresh property trials to maintain consistent performance across all mix variations while ensuring compatibility with the sand recycled materials.

II.1.7 Waste Glass Powder (WGP)

Waste glass powder was produced from post-consumer clear glass bottles collected from local recycling facilities. The glass was initially sorted and cleaned to remove labels, caps, and other contaminants. Following cleaning, the glass underwent a two-stage crushing process: primary crushing using a jaw crusher to reduce particle size to approximately 5 mm, followed by ball milling to achieve the target fineness. The grinding process was controlled to ensure 95% of particles passed through a 75 µm sieve, consistent with established recommendations for pozzolanic reactivity optimization [33], [34]. This fine particle size promotes the pozzolanic reaction between the amorphous silica in glass powder and calcium hydroxide produced during cement hydration, while minimizing the risk of deleterious alkali-silica reaction. The detailed chemical composition of the waste glass powder is summarized in Table 6, indicating that the material

contained approximately 72.6% SiO_2, 13.24% Na_2O, 10.42% CaO, and trace amounts of other oxides. The high silica content and amorphous structure contribute to the pozzolanic properties of the material. Physical properties including specific gravity (2.62 g/cm³) and particle size distribution were characterized using standard laboratory procedures. The processed glass powder was stored in sealed containers to prevent moisture absorption and maintain consistent properties throughout the experimental program. Prior to use, the material was verified to be free from organic contaminants and exhibited uniform color and texture characteristics. Figure 4 shows the Waste Glass Powder used.

Table 6: Chemical composition of waste glass powder (WGP).

Material	SiO_2	Fe_2O_3	Al_2O_3	CaO	TiO_2	MgO	Na_2O	K_2O	LOI
Glass Powder	72.6	0.4	1.5	10.42	0.04	1.2	13.24	0.5	0.55

Source: Authors, (2025).

Figure 4: Waste glass powder (≤75 μm).
Source: Authors, (2025).

III. EXPERIMENTAL PROGRAM

III.1 MIXTURE DESIGN APPROACH

The experimental investigation employed an I-optimal mixture design to systematically evaluate the combined effects of waste glass powder (WGP), recycled sand (RS), and steel fibers (SF) on the fresh and hardened properties of self-compacting concrete. This design methodology was selected based on its superior predictive capability and efficiency in capturing complex interactions among mixture constituents while minimizing prediction variance across the experimental domain. Unlike conventional factorial designs, mixture designs inherently account for the dependency among components where the sum of constituent proportions equals unity, mathematically expressed as:

$$\sum_{i=1}^{n} X_i = 1 \quad (1)$$

Where Xi represents the proportion of the i-th variable component [35]. Unlike conventional factorial designs that treat factors independently, mixture designs inherently account for the constraint that variable proportions must sum to unity, providing a more realistic framework for concrete mixture optimization within the defined experimental space.

The I-optimal criterion was specifically chosen over D-optimal or A-optimal alternatives due to its focus on maximizing prediction accuracy rather than parameter estimation precision or average prediction variance. This approach distributes design points optimally across the constrained mixture space, providing balanced information for model estimation while ensuring efficient exploration of both main effects and interaction terms [36]. The criterion is particularly advantageous when the primary objective is developing predictive models for practical applications rather than purely statistical inference.

The experimental framework maintained several parameters constant to isolate the effects of the three studied variables: total binder content at 400 kg/m³, water-to-binder ratio of 0.42, and superplasticizer dosage at 2.45% by cement mass. This approach enabled clear attribution of performance variations to the specific influence of WGP, RS, and SF combinations.

III.2 EXPERIMENTAL MATRIX AND FACTOR RANGES

The experimental program comprised forty-four concrete mixtures generated using Design-Expert®13 software (Stat-Ease, Inc.), incorporating both unique factorial combinations and strategically placed replicate points for pure error estimation. Factor levels were established through comprehensive literature review and preliminary laboratory trials to ensure both scientific rigor and practical feasibility for SCC production [37].

The selected variable ranges were defined as follows:

Waste Glass Powder (WGP): Cement replacement levels of 0%, 5%, 10%, 15%, and 20% by mass. This range reflects optimal balance between pozzolanic enhancement and potential early-age strength reduction. Literature evidence indicates that finely ground

glass powder (< 75 μm) exhibits significant pozzolanic activity while minimizing alkali-silica reaction risks at replacement levels up to 20% [38], [39]. Higher replacement ratios were avoided to prevent excessive early-age strength loss and delayed expansion concerns.

Recycled Sand (RS): Natural sand replacement at 0%, 15%, 30%, 45%, and 60% by mass. These levels represent practical scenarios for recycled aggregate utilization in SCC applications. The upper limit of 60% reflects the maximum feasible replacement that maintains acceptable fresh and hardened properties when supported by appropriate mix design adjustments [40], [41]. This range balances sustainability objectives with performance requirements.

Steel Fibers (SF): Volume fractions of 0%, 0.3%, 0.6%, 0.9%, and 1.2%. These dosages align with established recommendations for fiber-reinforced SCC, where fibers enhance post-cracking behavior without severely compromising workability [42–44]. The 1.2% upper limit prevents fiber balling phenomena and ensures uniform dispersion during mixing operations.

All mixtures maintained consistent water-to-cement ratio of 0.42 and cement content of 400 kg/m³, resulting in water content of 168 kg/m³. Polycarboxylate-based superplasticizer (MEDAPLAST SP 40) was incorporated at 2.45% by cement mass to achieve required flowability while preserving mixture stability.

The experimental matrix was generated using Design-Expert®13 software (Stat-Ease, Inc.), which provided specialized algorithms for mixture design and response surface methodology. The I-optimal algorithm strategically distributed the forty-four experimental points throughout the constrained mixture space, including replicated configurations to enable pure error estimation for lack-of-fit testing. This software-based approach enabled systematic optimization of mixture proportions, construction of polynomial regression models, and visualization of response surfaces, providing a robust analytical framework for examining interactions among WGP, RS, and SF while ensuring reliable detection of curvature effects and interaction terms essential for accurate response surface modeling.

III.3 MIX DESIGN AND PROPORTIONING

The mixture proportioning methodology was designed to maintain consistent baseline conditions while systematically varying the three target parameters. The following components remained constant across all formulations:

- Total binder content: 400 kg/m³ (cement + WGP)
- Water-to-binder ratio: 0.42 (considering WGP as active binder)
- Superplasticizer dosage: 2.45% by cement mass
- Total aggregate volume: maintained on absolute volume basis

WGP replaced cement on a direct mass substitution basis while maintaining total binder content at 400 kg/m³. This approach recognizes the pozzolanic contribution of finely ground glass powder to long-term strength development. RS replacement followed mass-for-mass substitution of natural sand according to designated percentages. Steel fibers were incorporated volumetrically, with corresponding reduction in 8/16 mm coarse aggregate mass to maintain constant paste volume and mixture balance. The 3/8 mm gravel fraction remained constant at 270.3 kg/m³ throughout all formulations.

This systematic proportioning strategy ensured that observed variations in concrete properties could be directly attributed to WGP, RS, and SF influences rather than inconsistencies in overall mixture composition, providing a reliable foundation for evaluating individual and interactive effects on SCC performance.

III.4 COMPLETE EXPERIMENTAL MATRIX

Table 7 presents the comprehensive experimental matrix detailing the proportions of WGP, RS, and SF for each mixture, along with calculated quantities of all constituents. The table includes both the percentage levels of variable components and absolute quantities (kg/m³) of all mixture constituents, ensuring complete reproducibility of the experimental program.

III.5 SPECIMEN PREPARATION AND CURING

All concrete mixtures were prepared in a 100-L vertical-shaft pan mixer under controlled laboratory conditions (20 ± 2 °C, 65 ± 5% RH) following a standardized sequence to ensure batch consistency. Cement, waste glass powder (WGP), and aggregates were first dry-blended for 2 minutes, after which steel fibers were gradually added and mixed for 1 minute to prevent clustering. Approximately two-thirds of the mixing water was then introduced and mixed for 2 minutes, followed by the remaining water pre-dissolved with a polycarboxylate superplasticizer and mixed for 3 minutes until a cohesive, self-compacting consistency was achieved.

Fresh concrete was cast into steel molds without external vibration, relying on its inherent self-compacting ability. After 24 hours under laboratory conditions, specimens were demolded and cured in water at 20 ± 2 °C until testing. This preparation and curing procedure ensured reproducibility and provided a robust basis for assessing the effects of WGP, recycled sand (RS), and steel fibers (SF) on both fresh and hardened properties of self-compacting concrete.

Table 7: Experimental matrix : proportions of WGP, RS, and SF with fixed binder and aggregate contents.

Mix No.	WGP	RS	SF	Cement	Sand		Gravel		WGP	Water
					Natural	Recycled	3/8	8/16		
	(%)	(%)	(%)	(kg/m³)	(kg/m³)	(kg/m³)	(kg/m³)	(kg/m³)	(kg/m³)	(kg/m³)
1	0	0	0	400.0	820.0	0.0	270.3	540.6	0.0	168.0
2	5	0	0	380.0	820.0	0.0	270.3	540.6	20.0	168.0
3	10	0	0	360.0	820.0	0.0	270.3	540.6	40.0	168.0
4	15	0	0	340.0	820.0	0.0	270.3	540.6	60.0	168.0
5	20	0	0	320.0	820.0	0.0	270.3	540.6	80.0	168.0
6	0	15	0	400.0	697.0	123.0	270.3	540.6	0.0	168.0

7	0	30	0	400.0	574.0	246.0	270.3	540.6	0.0	168.0
8	0	45	0	400.0	451.0	369.0	270.3	540.6	0.0	168.0
9	0	60	0	400.0	328.0	492.0	270.3	540.6	0.0	168.0
10	0	0	0.3	400.0	820.0	0.0	270.3	532.6	0.0	168.0
11	0	0	0.6	400.0	820.0	0.0	270.3	524.6	0.0	168.0
12	0	0	0.9	400.0	820.0	0.0	270.3	516.6	0.0	168.0
13	0	0	1.2	400.0	820.0	0.0	270.3	508.6	0.0	168.0
14	10	30	0.6	360.0	574.0	246.0	270.3	524.6	40.0	168.0
15	10	30	0	360.0	574.0	246.0	270.3	540.6	40.0	168.0
16	10	30	1.2	360.0	574.0	246.0	270.3	508.6	40.0	168.0
17	10	0	0.6	360.0	820.0	0.0	270.3	524.6	40.0	168.0
18	10	60	0.6	360.0	328.0	492.0	270.3	524.6	40.0	168.0
19	0	30	0.6	400.0	574.0	246.0	270.3	524.6	0.0	168.0
20	20	30	0.6	320.0	574.0	246.0	270.3	524.6	80.0	168.0
21	5	15	0	380.0	697.0	123.0	270.3	540.6	20.0	168.0
22	15	45	0	340.0	451.0	369.0	270.3	540.6	60.0	168.0
23	0	15	0.3	400.0	697.0	123.0	270.3	532.6	0.0	168.0
24	0	45	0.9	400.0	451.0	369.0	270.3	516.6	0.0	168.0
25	5	0	0.3	380.0	820.0	0.0	270.3	532.6	20.0	168.0
26	15	0	0.9	340.0	820.0	0.0	270.3	516.6	60.0	168.0
27	10	15	0.3	360.0	697.0	123.0	270.3	532.6	40.0	168.0
28	10	45	0.9	360.0	451.0	369.0	270.3	516.6	40.0	168.0
29	5	15	0.6	380.0	697.0	123.0	270.3	524.6	20.0	168.0
30	15	45	0.6	340.0	451.0	369.0	270.3	524.6	60.0	168.0
31	5	45	0.3	380.0	451.0	369.0	270.3	532.6	20.0	168.0
32	15	15	0.9	340.0	697.0	123.0	270.3	516.6	60.0	168.0
33	5	30	0.9	380.0	574.0	246.0	270.3	516.6	20.0	168.0
34	15	30	0.3	340.0	574.0	246.0	270.3	532.6	60.0	168.0
35	7.5	22.5	0.45	370.0	635.5	184.5	270.3	528.6	30.0	168.0
36	12.5	37.5	0.75	350.0	512.5	307.5	270.3	524.6	50.0	168.0
37	20	60	0	320.0	328.0	492.0	270.3	540.6	80.0	168.0
38	20	0	1.2	320.0	820.0	0.0	270.3	508.6	80.0	168.0
39	0	60	1.2	400.0	328.0	492.0	270.3	508.6	0.0	168.0
40	20	60	1.2	320.0	328.0	492.0	270.3	508.6	80.0	168.0

Source: Authors, (2025).

III.6 TESTING PROCEDURE

The experimental program was structured to comprehensively evaluate the fresh and hardened properties of steel fiber-reinforced self-compacting concrete incorporating waste glass powder (WGP) and recycled sand (RS).

Fresh concrete workability was assessed immediately after mixing using standardized SCC tests. The slump flow test (EN 12350-8) determined filling ability by measuring the average spread diameter in two perpendicular directions after lifting the cone. The V-funnel test (EN 12350-9) measured viscosity and segregation resistance through the flow time of concrete passing the V-shaped apparatus. Passing ability was evaluated by the J-ring test (EN 12350-12), comparing slump flow and J-ring flow diameters, and confirmed by the L-box test (EN 12350-10) through calculation of the blocking ratio (H_2/H_1).

All tests were completed within 15 minutes of mixing under controlled laboratory conditions (20 ± 2 °C, 65 ± 5% RH). Each measurement was conducted in triplicate, and mean values were reported when the variation among results was below 5%. This systematic protocol ensured reliable characterization of SCC workability in compliance with EFNARC guidelines [45]. Figure 5 depicts the fresh property testing setup used in the experimental program.

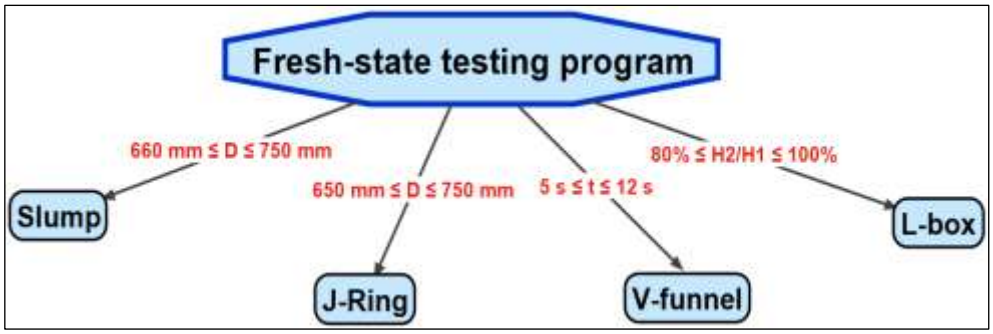

Figure 5: Fresh-state testing program for self-compacting concrete workability assessment.
Source: Authors, (2025).

The hardened performance of the mixtures was evaluated through a comprehensive program combining mechanical and durability assessments. Compressive strength was measured on 150 mm cubes at 28, 56, and 90 days in accordance with EN 12390-3. Specimens were demolded after 24 h and cured in water at 20 ± 2 °C until testing. For each age and mixture, the mean value of three specimens was reported to ensure statistical reliability.

Flexural strength was determined at 28 days using 100 × 100 × 400 mm prisms under a four-point bending setup following ASTM C78, with a controlled loading rate of 1.0 ± 0.3 MPa/min to maintain uniformity across batches. Durability was assessed at 90 days through capillary water absorption following ASTM C642. Oven-dried specimens (105 °C, constant mass) were exposed to unidirectional water ingress, and mass gain was recorded at specified intervals for 64 h. The sorptivity coefficient was calculated from the linear relationship between cumulative absorption and the square root of time.

This integrated methodology provided a robust basis for quantifying the effects of waste glass powder, recycled sand, and steel fibers on the mechanical and durability performance of self-compacting concrete. Figure 6 shows the testing setup and procedures for hardened property evaluation.

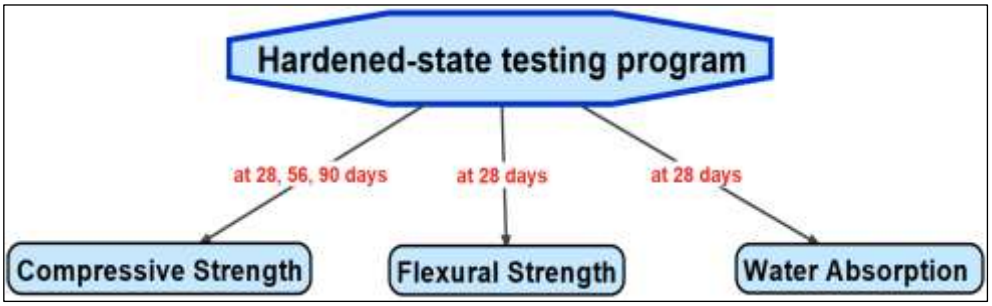

Figure 6: Hardened property evaluation setup for mechanical and durability characterization.
Source: Authors, (2025).

IV. RESULTS AND DISCUSSIONS

IV.1 MODEL DEVELOPMENT AND VALIDATION

The response surface methodology, implemented through the I-optimal mixture design, facilitated the development of statistically robust regression models describing the effects of waste glass powder (WGP), recycled sand (RS), and steel fibers (SF) on both the fresh and hardened properties of SCC. Quadratic polynomial functions were generally sufficient to capture the observed experimental trends, while cubic terms were introduced in specific cases—such as V-funnel and L-box tests—to better represent nonlinear flow behavior under restrictive conditions.

The predictive reliability of the models was demonstrated by coefficients of determination (R^2) ranging from 0.85 to 0.99, with adjusted R^2 values remaining closely aligned, confirming the absence of overfitting. Analysis of variance (ANOVA) further validated the statistical significance of all regression terms ($p < 0.0001$), while lack-of-fit tests were non-significant ($p > 0.05$), establishing the adequacy of the selected models.

Model adequacy was reinforced through diagnostic evaluations. Normal probability plots of residuals (Figure 7a and 7b) showed data points closely following a straight line, indicating normally distributed errors, while predicted versus experimental plots (Figure 8a and 8b) revealed strong correlations across all responses ($R^2 > 0.93$). These diagnostics confirm that the models not only meet statistical requirements but also capture the practical behavior of SCC mixtures under varying proportions of industrial by-products and fibers.

The complete regression equations, expressed in coded variables, are provided in Table 8 (fresh properties) and Table 9 (hardened properties). These tables consolidate the model forms, coefficients, and statistical indices, offering both a compact summary and a practical predictive framework. Collectively, the models provide a reliable tool for optimizing SCC mixtures, enabling engineers to balance workability, stability, and mechanical performance when incorporating recycled and supplementary materials.

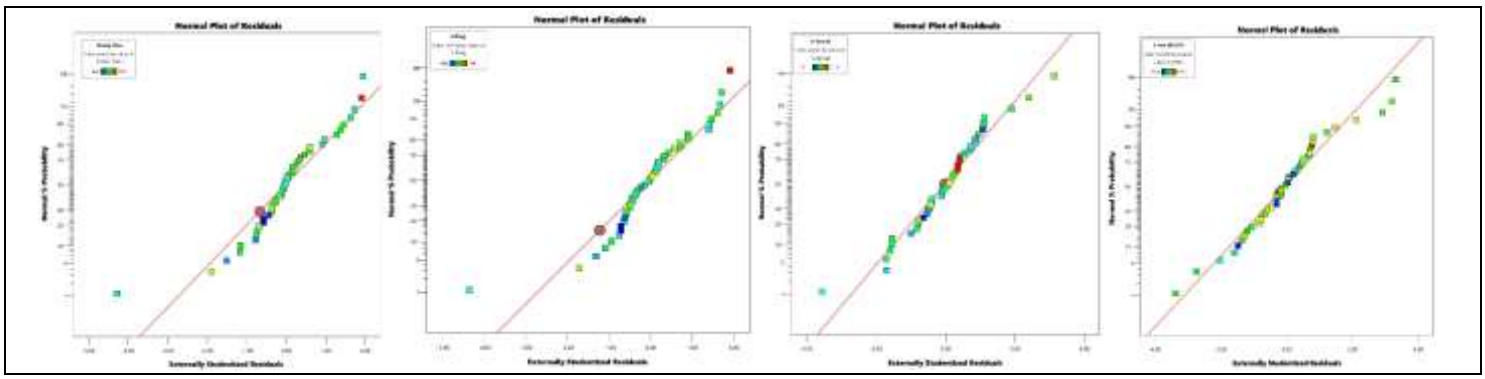

Figure 7a: Model validation diagnostics: Normal probability plots of residuals demonstrating adequate model fit for all response variables (fresh-state).
Source: Authors, (2025).

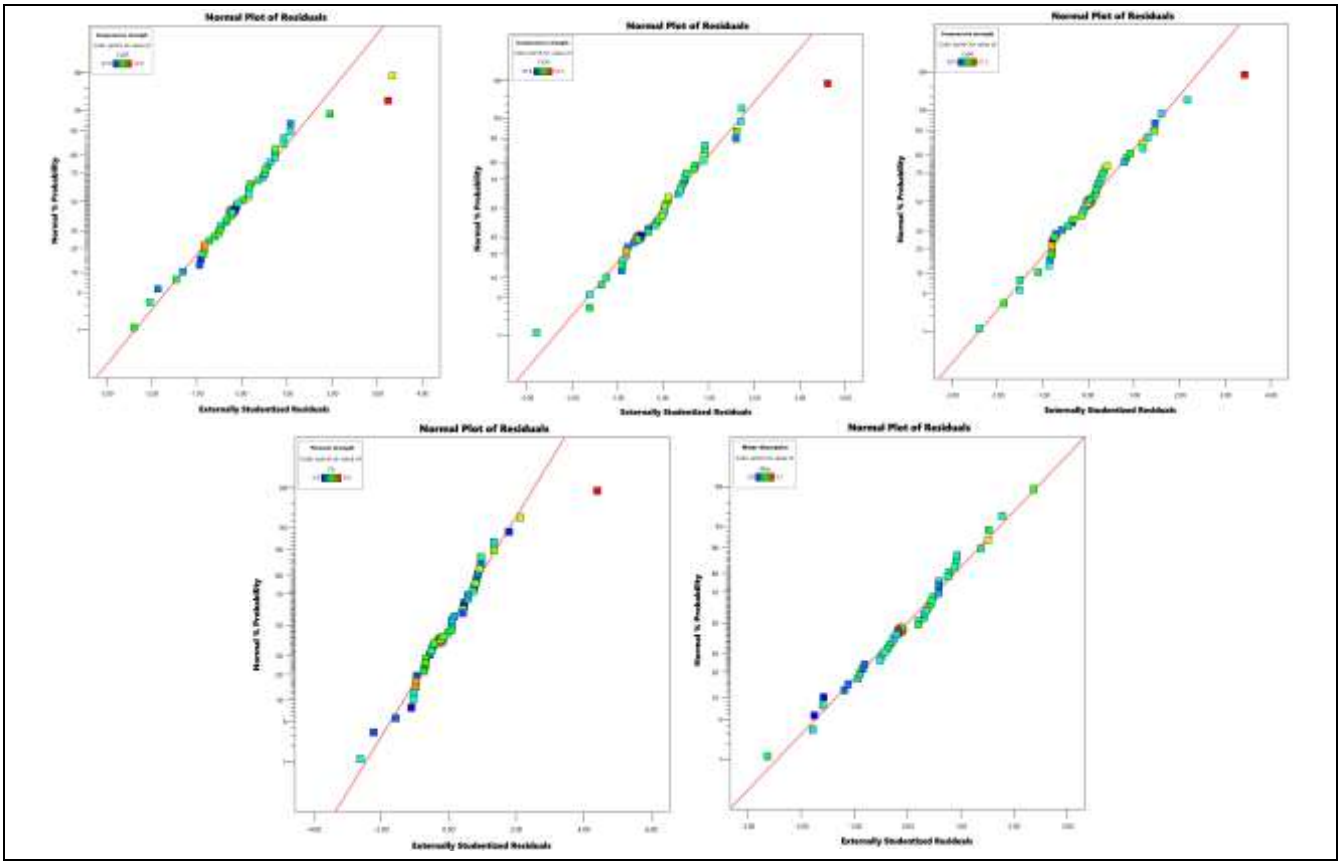

Figure 7b: Model validation diagnostics: Normal probability plots of residuals demonstrating adequate model fit for all response variables (hardened-state).
Source: Authors, (2025).

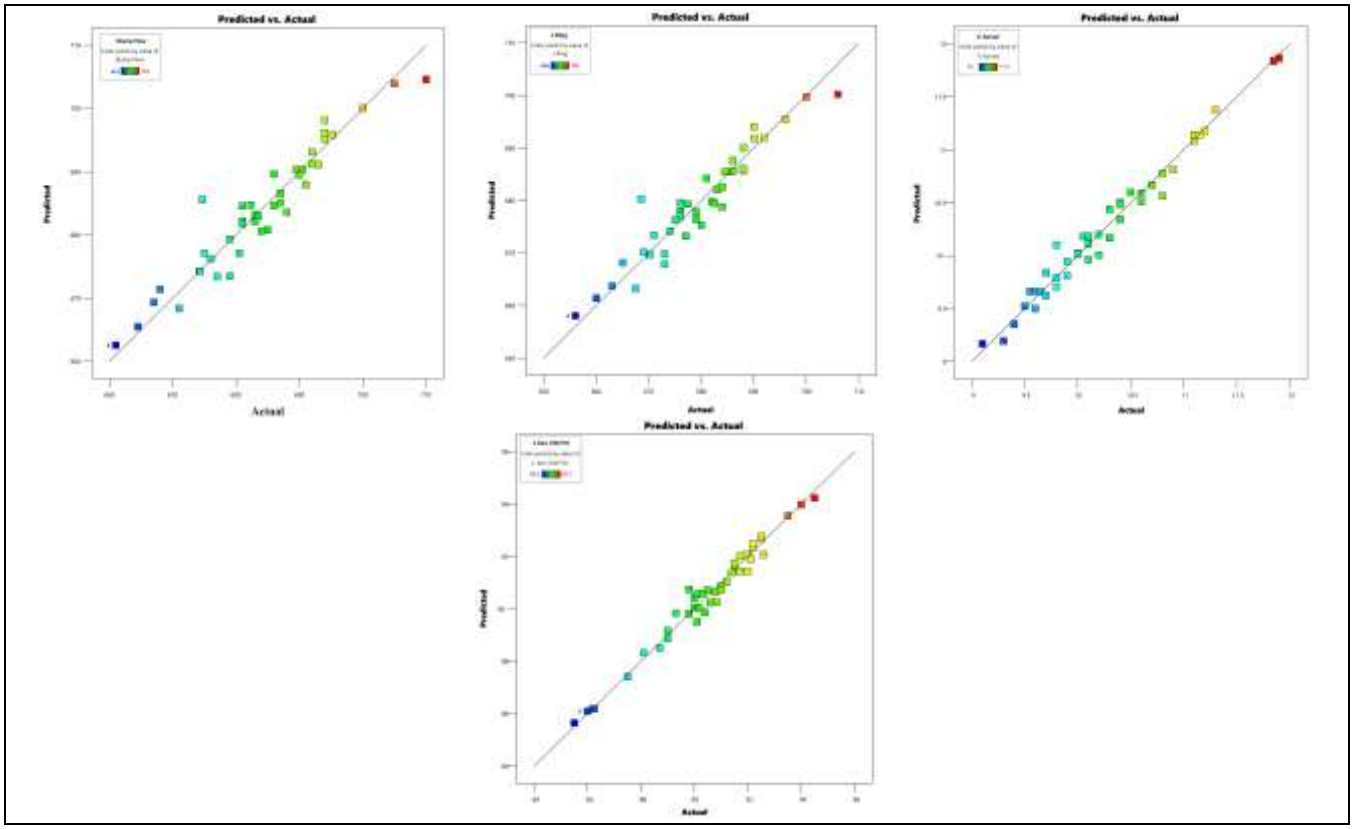

Figure 8a: Predicted versus actual correlations: (a-i) Model accuracy assessment across all measured properties with corresponding R^2 values (fresh-state).
Source: Authors, (2025).

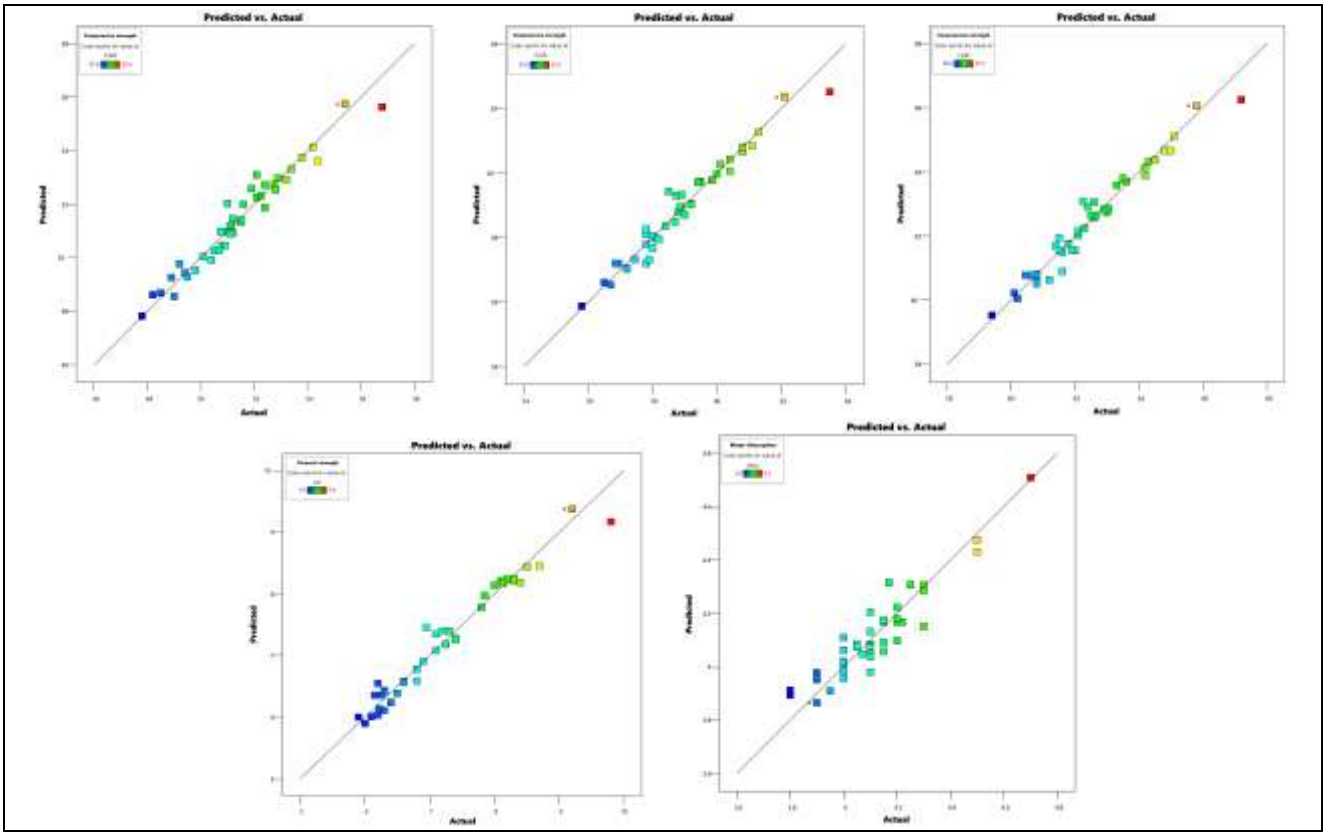

Figure 8b: Predicted versus actual correlations: (a-i) Model accuracy assessment across all measured properties with corresponding R^2 values (hardened-state).
Source: Authors, (2025).

Table 8: Regression models for the fresh-state properties of self-compacting concrete (SCC) incorporating waste glass powder (WGP), recycled sand (RS), and steel fibers (SF).

Response	Model Type	Regression Equation (coded variables)	F-value	R^2	Adj. R^2	Adeq. Precision
Slump Flow	Quadratic	$Y = 687.95 + 4.14A – 4.53B – 7.66C + 5.47BC – 10.34A^2$	47.20	0.9259	0.9063	26.82
J-Ring	Quadratic	$Y = 673.2 – 3.95A – 6.14B – 9.45C + 4.82BC – 8.90A^2$	41.71	0.9169	0.8950	25.32
V-Funnel	Cubic	$Y = 9.96 – 0.35A + 0.30B + 0.76C – 0.18AC – 0.29BC + 0.29A^2 + 0.34B^2 + 0.23C^2$	15.82	0.9507	0.9377	28.45
L-Box	Cubic	$Y = 0.91 – 0.01A – 0.02B – 0.05C + 0.02BC – 0.03C^2$	56.34	0.9021	0.8794	23.65

Source: Authors, (2025).

A = WGP (%), B = RS (%), C = SF (%); All models showed statistical significance ($p < 0.0001$).

Table 9: Regression models for the hardened-state properties of self-compacting concrete (SCC) incorporating waste glass powder (WGP), recycled sand (RS), and steel fibers (SF).

Response	Model Type	Regression Equation (coded variables)	F-value	R^2	Adj. R^2	Adeq. Precision
Compressive Strength (28d)	Quadratic	$Y = 52.03 – 0.36A – 0.52B + 3.26C – 0.33BC – 0.35B^2 – 0.33C^2$	26.29	0.9	0.8735	22.45
Compressive Strength (56d)	Cubic	$Y = 59.31 + 0.38A - 0.36B + 3.08C - 0.14AB - 0.70AC + 0.01BC - 0.12A^2 - 0.06B^2 - 0.22C^2$	31.78	0.9618	0.9315	27.43
Compressive Strength (90d)	Cubic	$Y = 63.06 + 0.63A – 0.38B + 3.20C – 0.65AC + 3.90ABC – 0.27C^2$	33.64	0.9638	0.9352	25.69
Flexural Strength	Cubic	$Y = 7.35 + 0.15A – 0.13B + 1.79C – 0.12AC$	36.30	0.9664	0.9397	30.64
Water Absorption	Quadratic	$Y = 4.02 – 0.047A + 0.16B – 0.16C – 0.057BC + 0.13B^2$	25.53	0.8715	0.8375	21.34

Source: Authors, (2025).

Coded variables: A = (WGP - 10)/10, B = (RS - 30)/30, C = (SF - 0.6)/0.6

IV.2 FRESH PROPERTIES

The fresh properties of SCC exhibited clear sensitivity to variations in WGP, RS, and SF. The following subsections present the individual test results, supported by response surface analyses, to elucidate the influence of mixture parameters on flowability, passing ability, and segregation resistance.

IV.2.1 Slump Flow

The slump flow test demonstrated that steel fiber (SF) content exerted the strongest influence on the workability of SCC mixtures. Regression analysis (Table 8) confirmed its dominant role, accounting for 21.9% of the model sum of squares ($F = 100.28$, $p < 0.0001$). Each 0.3% increment in fiber dosage consistently reduced slump flow diameter by approximately 25–30 mm. This reduction is primarily attributed to increased interparticle friction and mechanical blocking caused by fiber interlocking, a phenomenon widely reported in previous investigations [42], [46], [47]. From a practical perspective, this finding underscores the trade-off between the mechanical benefits of fibers and their adverse effect on flowability, an important consideration in the design of SCC for heavily reinforced structures.

A significant RS × SF interaction ($F = 38.73$, $p < 0.0001$) further revealed that the combined incorporation of recycled sand (RS) and fibers mitigated flow reduction compared to the expected additive effect of each factor alone. This compensating mechanism suggests that the angular particle geometry of RS may facilitate more efficient packing and particle rearrangement, thereby offsetting part of the flow restriction induced by fibers. Such synergy not only enhances mixture stability but also offers practical advantages when designing SCC with multiple waste-derived constituents.

Waste glass powder (WGP) also showed a notable influence on slump flow. At moderate replacement levels (≈12–15%), WGP improved flowability due to its filler effect and smooth particle morphology, which enhanced paste rheology and reduced internal friction. However, beyond this threshold, a significant quadratic effect (coefficient ≈ –10.34) was observed, leading to reduced flowability as a consequence of increased surface area and higher water demand. This nonlinear behavior confirms the presence of an optimal WGP content, beyond which the benefits are outweighed by rheological limitations. The trend aligns with earlier studies that have identified similar dosage thresholds for glass powder in SCC systems.

Figure 9 presents the response surface illustrating how waste glass powder and recycled sand jointly influence slump flow when steel fiber content remains fixed at 0.6%. The data indicate that flowability reaches its peak values (690-710 mm) within a relatively narrow window: WGP replacements between 5-12% paired with moderate recycled sand usage (15-30%). qWhen both materials exceed these ranges simultaneously, slump flow decreases noticeably. This pattern reflects how each material contributes to mixture thickening through different mechanisms - WGP through increased surface area at higher dosages, and recycled sand through its inherently higher water absorption and angular particle texture. Such findings underscore the critical balance required when incorporating multiple waste streams into self-compacting concrete formulations.

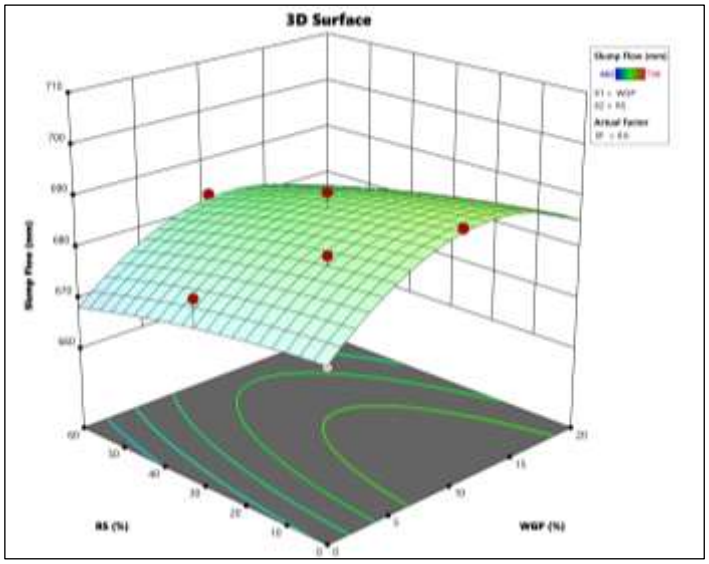

Figure 9: Interactive effects of waste glass powder and recycled sand on concrete flowability represented through three-dimensional response surface modeling.
Source: Authors, (2025).

The contour plot (Figure 10) offers a different perspective on the same data, making it easier to identify specific operating windows for mixture design. Two distinct zones emerge from this analysis: an optimal region where slump flow exceeds 700 mm, and areas where performance deteriorates rapidly.

The high-performance zone appears quite narrow, confined to combinations where WGP stays below 10% while recycled sand ranges between 15-30%. Beyond these boundaries, particularly when WGP content rises above 15%, flowability drops sharply regardless of the recycled sand level. Similarly, recycled sand proportions exceeding 45% consistently undermine workability, even with minimal glass powder addition.

These patterns suggest that each material imposes its own threshold beyond which the benefits reverse into drawbacks. For practical mixture design, this mapping helps engineers avoid problematic combinations while identifying the sweet spot for achieving both sustainability goals and workability requirements.

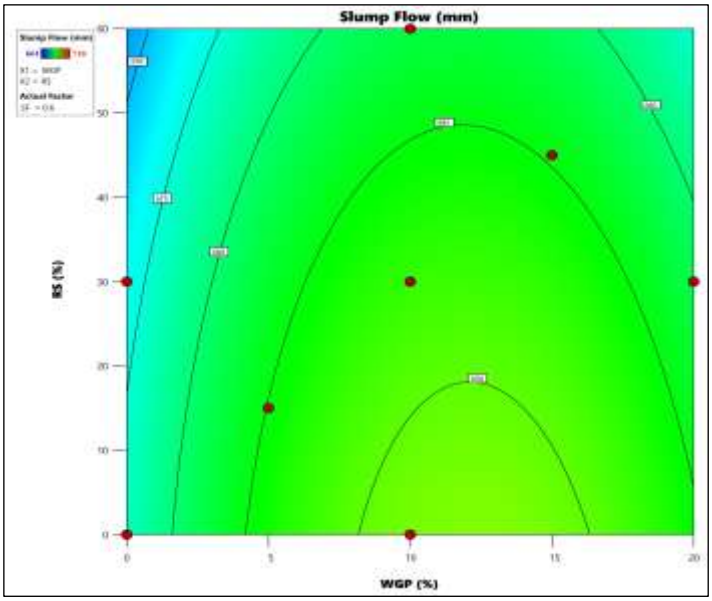

Figure 10: Contour representation of slump flow response revealing optimal mixture proportions for waste glass powder and recycled sand combinations.
Source: Authors, (2025).

IV.2.2 V-Funnel Flow Characteristics

The V-funnel test required a cubic regression model to capture the nonlinear flow behavior of SCC mixtures, achieving an excellent fit (R^2 = 0.9507). Flow times ranged from 8.2 s in the fiber-free control mix to 12.5 s at the highest fiber dosage (1.2%), clearly demonstrating the strong influence of steel fibers on mixture viscosity and segregation resistance. This marked increase reflects a transition from nearly Newtonian to distinctly non-Newtonian flow behavior, as fiber networks progressively develop within the fresh matrix. These results corroborate the observations of Roussel (2006), who reported similar rheological transitions in fiber-reinforced SCC under increasing shear.

The cubic model was crucial for identifying threshold effects, particularly at low fiber dosages where small additions caused disproportionately large increases in flow resistance. This suggests the presence of a critical fiber content at which percolation networks begin to form, fundamentally altering flow dynamics. Waste glass powder (WGP) exerted a secondary but measurable influence, reducing flow times by roughly 8–12% at moderate replacement levels due to enhanced particle packing and improved lubrication. However, replacement levels beyond 15% reversed this benefit, likely due to increased specific surface area and water demand. Recycled sand (RS) consistently elevated flow times, surpassing EFNARC limits (>12 s) when replacement exceeded 45%, primarily as a result of higher water absorption and the angular particle morphology typical of recycled aggregates.

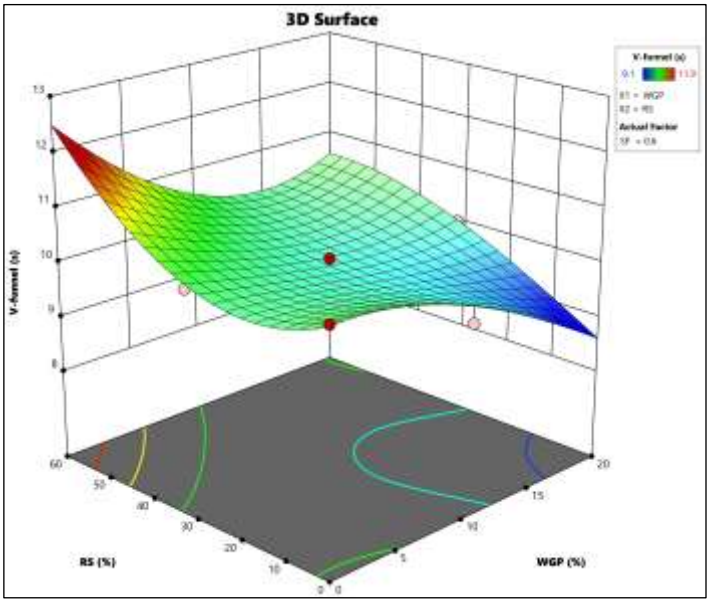

Figure 11: Response surface of V-funnel flow time showing nonlinear influence of steel fiber content.
Source: Authors, (2025).

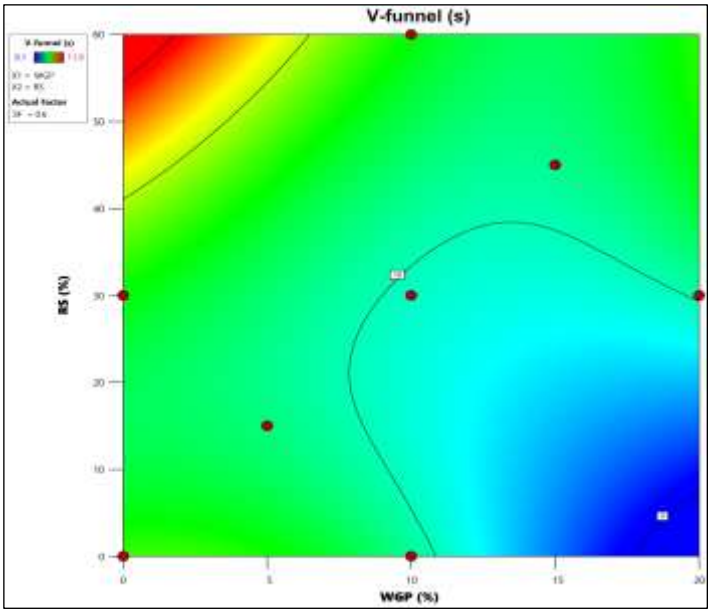

Figure 12: Contour map illustrating critical fiber thresholds required to maintain acceptable flow characteristics.
Source: Authors, (2025).

IV.2.3 J-Ring Performance

Passing ability is a key performance criterion for SCC, particularly in heavily reinforced elements. Both J-ring and L-box tests identified steel fiber dosage as the main factor restricting flow, though each test revealed different aspects of this limitation.

The J-ring model ($R^2 = 0.9169$) showed that each 0.3% increment of steel fibers reduced the J-ring spread by 15–20 mm compared with unconfined slump flow, reaching a maximum difference of approximately 50 mm at 1.2% fiber content. This reduction reflects the tendency of fibers to align around obstacles, forming bridging zones that hinder flow. Similar reductions were reported by Libre et al. (2011) in their investigation of hooked-end fibers.

Recycled sand further amplified these restrictions due to its angular shape and higher interparticle friction. Mixtures containing more than 60% RS consistently fell below recommended J-ring performance limits regardless of fiber dosage. Interestingly, moderate WGP levels (10–12%) mitigated this effect by improving paste lubrication and cohesion, leading to slightly higher J-ring spreads.

IV.2.4 L-Box

L-box results followed a similar trend but were even more sensitive to fiber content. Blocking ratios decreased from 0.95 in the control mix to 0.82 at 1.2% fiber dosage, approaching the EFNARC critical threshold of 0.80. The quadratic trend indicates that flow restriction accelerates at higher fiber contents, most likely due to intensified fiber–fiber interactions and network formation.

Critical combinations were observed when high fiber content was paired with elevated RS levels. For example, mixtures containing 1.0% SF and 45% RS produced blocking ratios of 0.79, slightly below EFNARC acceptance criteria. This confirms the multiplicative rather than additive nature of flow restrictions, consistent with the findings of Khayat et al. (2019), who reported similar compounded effects in fiber-reinforced SCC.

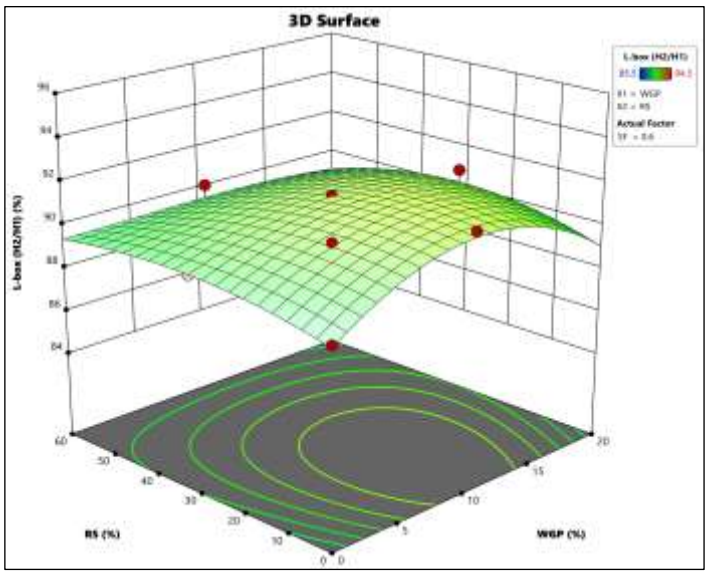

Figure 13: L-box blocking ratio response surface highlighting critical performance boundaries for fiber-reinforced SCC mixtures.
Source: Authors, (2025).

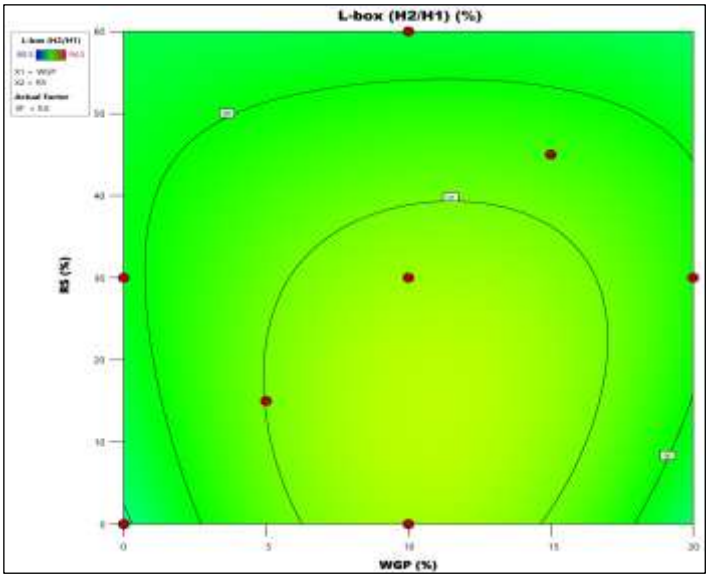

Figure 14: Optimization contours identifying acceptable design regions for sustainable SCC containing recycled materials.
Source: Authors, (2025).

IV.3 HARDENED PROPERTIES

IV.3.1 Compressive Strength Development

Compressive strength development reflected the combined effects of mechanical reinforcement from steel fibers and chemical enhancement from pozzolanic reactions. Early-Age Strength (28 Days), At 28 days, steel fiber content was the dominant factor (R^2 = 0.9000), with each 0.3% increment producing a 2.8–3.2 MPa strength gain. This enhancement is attributed to the crack-bridging capacity of fibers, which maintain load transfer across developing microcracks and delay crack propagation. These results align with the findings of Yazıcı et al. (2007), who reported comparable strength gains in high-performance concrete with hooked-end fibers.

WGP exhibited a slight negative coefficient (-0.36) at this age, reflecting the slower reactivity of glass powder compared to cement hydration. This early-age strength reduction has been reported by Shi et al. (2005) and is attributed to the time required for secondary C–S–H formation. RS replacement showed a predictable negative influence (-0.52 MPa per 15% replacement), consistent with the weaker interfacial transition zones typically associated with recycled aggregates (Evangelista and de Brito, 2007).

Intermediate-Age Development (56 Days), By 56 days, the pozzolanic contribution of WGP became evident, with positive coefficients (+0.38 MPa) and visible strength improvements. The optimal mix (15% WGP, 50% RS, 1.0% SF) reached 59.7 MPa, a 24% increase compared with the control. This demonstrates a synergistic interaction between fiber reinforcement and secondary hydration, which progressively densifies the matrix. Long-Term Strength (90 Days), At 90 days, the WGP effect increased further (+0.63 MPa), with the optimal mixture achieving 64.8 MPa, representing a 28% improvement over control. These results confirm the substantial pozzolanic contribution of WGP and align with the findings of Rashad (2014), who documented significant long-term strength gains in glass powder concrete.

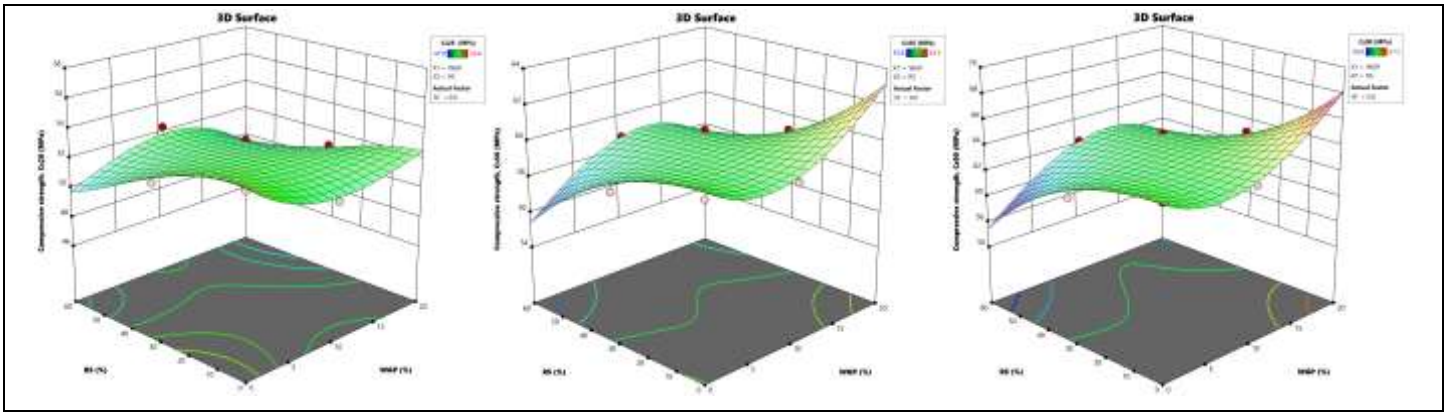

Figure 15: Response surfaces showing early-age fiber dominance, 56-day WGP activation, and 90-day strength improvement trends.
Source: Authors, (2025).

IV.3.2 Flexural Strength

Flexural strength analysis achieved excellent model accuracy (R^2 = 0.9276). Steel fiber content was the most significant factor (+1.79 MPa), with the optimal mix achieving 8.7 MPa at 28 days—a 38% increase over the control mixture. This demonstrates the ability of hooked-end fibers to transform brittle failure into pseudo-ductile behavior, consistent with the mechanism described by Naaman (2003).

WGP provided a minor positive contribution (+0.15), while RS showed minimal negative impact (-0.13). The limited influence of these materials indicates that fiber reinforcement can compensate for matrix weakening effects, supporting the use of multiple sustainable constituents without compromising structural performance.

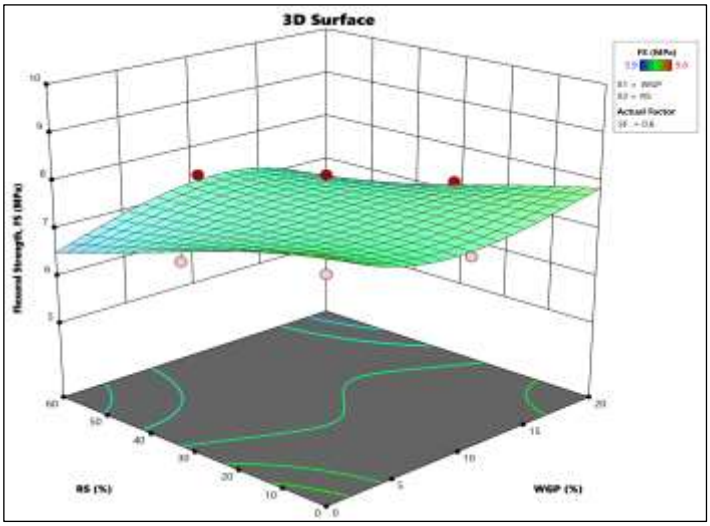

Figure 16: Response surface highlighting the dominant influence of steel fibers on flexural performance.
Source: Authors, (2025).

IV.3.3 Water absorption

Water absorption testing at 90 days (R^2 = 0.8715) revealed RS as the primary factor influencing permeability. Each 15% replacement increased absorption by 0.15–0.20% [48], due to the higher porosity and microcracking typical of recycled aggregates (Tam et al., 2018). WGP had a beneficial effect (-0.047 per 15% replacement) through matrix densification driven by pozzolanic reaction products. Steel fibers also reduced absorption (-0.164) by controlling crack formation and limiting pathways for fluid ingress, confirming the findings of Banthia and Gupta (2006). The optimal mix achieved 3.8% water absorption at 90 days, 15% lower than the control, placing it in the "excellent" category according to ACI 201.2R guidelines.

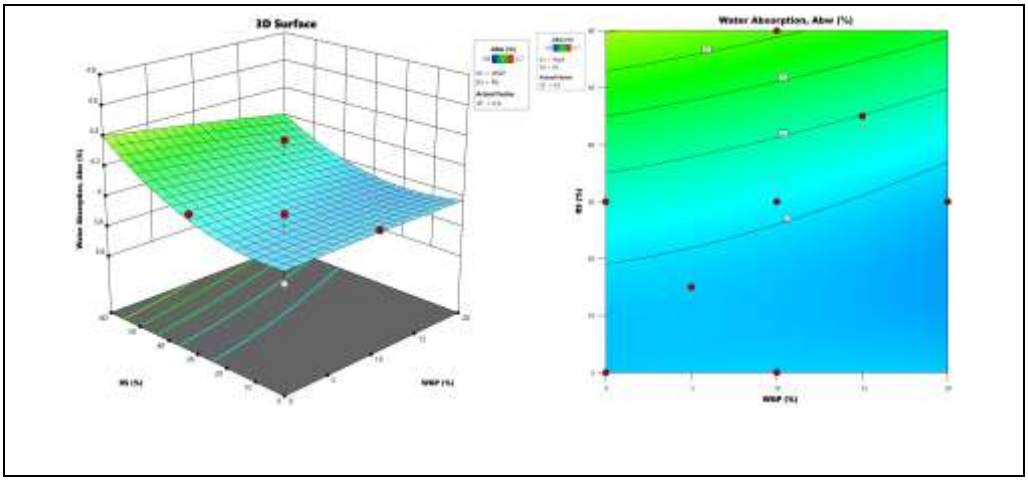

Figure 17: Response surface and optimization contours for durability performance.
Source: Authors, (2025).

V. CONCLUSIONS

This study systematically investigated the combined influence of waste glass powder (WGP), recycled sand (RS), and steel fibers (SF) on the fresh and hardened performance of self-compacting concrete (SCC) through response surface methodology. Results confirmed that partial cement replacement with WGP up to 15% enhanced workability and long-term strength through filler and pozzolanic effects, while RS replacement up to 50% maintained flowability within EFNARC limits when mix adjustments accounted for its higher absorption. Incorporation of 1.0% SF by volume markedly increased flexural strength and improved ductility without compromising self-compaction. Synergistic interactions between RS and SF produced compensatory effects that stabilized fresh properties and improved mechanical response, highlighting the importance of integrated mix design rather than isolated material contributions. The optimized mixture (15% WGP, 15% RS, 0.9% SF) achieved high compressive strength (53.4 MPa at 28 days, 64.8 MPa at 90 days), superior flexural performance, and reduced water absorption, reflecting improved matrix densification. The developed regression models ($R^2 > 0.92$) offer reliable predictive tools for practical mixture optimization. Overall, the findings demonstrate that carefully proportioned waste-derived constituents can deliver sustainable, high-performance SCC, supporting circular economy objectives while meeting modern durability and workability requirements.

VI. AUTdHOR'S CONTRIBUTION

Conceptualization: Souhila Fergani, Said Zaouai, Rachid Rabehi and Ali Abbache.
Methodology: Souhila Fergani, Said Zaouai, Rachid Rabehi and Ali Abbache.
Investigation: Souhila Fergani, Said Zaouai, Rachid Rabehi and Ali Abbache.
Discussion of results: Souhila Fergani, Said Zaouai, Rachid Rabehi and Ali Abbache.
Writing – Original Draft: Souhila Fergani, Said Zaouai, Rachid Rabehi and Ali Abbache.
Writing – Review and Editing: Souhila Fergani, Said Zaouai, Rachid Rabehi and Ali Abbache.
Resources: Souhila Fergani, Said Zaouai, Rachid Rabehi and Ali Abbache.
Supervision: Souhila Fergani, Said Zaouai, Rachid Rabehi and Ali Abbache.
Approval of the final text: Souhila Fergani, Said Zaouai, Rachid Rabehi and Ali Abbache.

VII. REFERENCES

[1] M. Sandanayake, G. Zhang, S. Setunge, Estimation of environmental emissions and impacts of building construction – A decision making tool for contractors, Journal of Building Engineering 21 (2019) 173–185. https://doi.org/10.1016/j.jobe.2018.10.023.

[2] M. Schneider, The cement industry on the way to a low-carbon future, Cement and Concrete Research 124 (2019) 105792. https://doi.org/10.1016/j.cemconres.2019.105792.

[3] M. Bendixen, L.L. Iversen, J. Best, D.M. Franks, C.R. Hackney, E.M. Latrubesse, L.S. Tusting, Sand, gravel, and UN Sustainable Development Goals: Conflicts, synergies, and pathways forward, One Earth 4 (2021) 1095–1111. https://doi.org/10.1016/j.oneear.2021.07.008.

[4] C.R. Rusnak, Sustainable Strategies for Concrete Infrastructure Preservation: A Comprehensive Review and Perspective, Infrastructures 10 (2025) 99. https://doi.org/10.3390/infrastructures10040099.

[5] H. Okamura, M. Ouchi, Self-Compacting Concrete, ACT 1 (2003) 5–15. https://doi.org/10.3151/jact.1.5.

[6] Said Mohammed Mostafa Aljamala, N.A. Safiee, N.A. Mohd Nasir, F.N.A. Abdul Aziz, Performance of Recycling Aggregate Self-Compacting Concrete Incorporating Supplementary Cementitious Materials: An Overview, JST 33 (2025). https://doi.org/10.47836/pjst.33.S4.08.

[7] L. Prasittisopin, W. Tuvayanond, T.H.-K. Kang, S. Kaewunruen, Concrete Mix Design of Recycled Concrete Aggregate (RCA): Analysis of Review Papers, Characteristics, Research Trends, and Underexplored Topics, Resources 14 (2025) 21. https://doi.org/10.3390/resources14020021.

[8] R. Rabehi, M. Rabehi, M. Omrane, Physical-mechanical and fresh state properties of self-compacting concrete based on different types of gravel reinforced with steel fibers: Experimental study and modeling, Construction and Building Materials 390 (2023) 131758. https://doi.org/10.1016/j.conbuildmat.2023.131758.

[9] C. Shi, Y. Wu, C. Riefler, H. Wang, Characteristics and pozzolanic reactivity of glass powders, Cement and Concrete Research 35 (2005) 987–993. https://doi.org/10.1016/j.cemconres.2004.05.015.

[10] A.A. Aliabdo, A.E.M. Abd Elmoaty, A.Y. Aboshama, Utilization of waste glass powder in the production of cement and concrete, Construction and Building Materials 124 (2016) 866–877. https://doi.org/10.1016/j.conbuildmat.2016.08.016.

[11] X. Jiang, R. Xiao, Y. Bai, B. Huang, Y. Ma, Influence of waste glass powder as a supplementary cementitious material (SCM) on physical and mechanical properties of cement paste under high temperatures, Journal of Cleaner Production 340 (2022) 130778. https://doi.org/10.1016/j.jclepro.2022.130778.

[12] M. Mejdi, W. Wilson, M. Saillio, T. Chaussadent, L. Divet, A. Tagnit-Hamou, Investigating the pozzolanic reaction of post-consumption glass powder and the role of portlandite in the formation of sodium-rich C-S-H, Cement and Concrete Research 123 (2019) 105790. https://doi.org/10.1016/j.cemconres.2019.105790.

[13] S. Ramírez-Arellanes, F. Montejo-Alvaro, H. Cruz-Martínez, H. Rojas-Chávez, J.M. Mendoza-Rangel, V.A. Franco-Luján, Pozzolanic Assessment of Recycled Waste Glass for Use as a Supplementary Cementitious Material, Construction Materials 5 (2025) 59. https://doi.org/10.3390/constrmater5030059.

[14] A.M. Matos, T. Ramos, S. Nunes, J. Sousa-Coutinho, Durability Enhancement Of SCC With Waste Glass Powder, Mat. Res. 19 (2016) 67–74. https://doi.org/10.1590/1980-5373-MR-2015-0288.

[15] E. Pahsha, P.S. Nair, R. Gupta, V. Agrawal, Sustainable development of self-compacting concrete incorporating granite waste and recycled concrete aggregate: Evaluation of strength, durability, and microstructure, Sustainable Chemistry and Pharmacy 47 (2025) 102136. https://doi.org/10.1016/j.scp.2025.102136.

[16] N. Garcia-Troncoso, L. Li, Q. Cheng, K.H. Mo, T.-C. Ling, Comparative study on the properties and high temperature resistance of self-compacting concrete with various types of recycled aggregates, Case Studies in Construction Materials 15 (2021) e00678. https://doi.org/10.1016/j.cscm.2021.e00678.

[17] M. Contreras Llanes, M. Romero Pérez, M.J. Gázquez González, J.P. Bolívar Raya, Construction and demolition waste as recycled aggregate for environmentally friendly concrete paving, Environ Sci Pollut Res 29 (2022) 9826–9840. https://doi.org/10.1007/s11356-021-15849-4.

[18] J. Ahmad, Z. Zhou, A.F. Deifalla, Steel Fiber Reinforced Self-Compacting Concrete: A Comprehensive Review, Int J Concr Struct Mater 17 (2023) 51. https://doi.org/10.1186/s40069-023-00602-7.

[19] M. Zhang, J. Chen, J. Liu, H. Yin, Y. Ma, F. Yang, Fracture Behavior of Steel-Fiber-Reinforced High-Strength Self-Compacting Concrete: A Digital Image Correlation Analysis, Materials 18 (2025) 3631. https://doi.org/10.3390/ma18153631.

[20] S. Thakur, U. Jhakal, P. Anand, P.N. Bhowmik, Synergistic use of recycled aggregates and waste glass powder for sustainable concrete: mechanical properties, durability performance, and microstructural insights, Asian J Civ Eng (2025). https://doi.org/10.1007/s42107-025-01483-9.

[21] A. Mardani, D. Hatungimana, N. Mardani, J. Assaad, H. El-Hassan, Feasibility of steel fiber-reinforced self-compacting concrete containing recycled aggregates – compliance with EFNARC guidelines, International Journal of Sustainable Engineering 18 (2025) 2538858. https://doi.org/10.1080/19397038.2025.2538858.

[22] S. Barbhuiya, B.B. Das, D. Adak, K. Kapoor, M. Tabish, Low carbon concrete: advancements, challenges and future directions in sustainable construction, Discov. Concr. Cem. 1 (2025) 3. https://doi.org/10.1007/s44416-025-00002-y.

[23] Z. Zhang, Y. Lei, J.Y.R. Liew, M. Liu, G. Wong, H. Du, Embodied carbon saving potential of using recycled materials as cement substitute in Singapore's buildings, Npj Mater. Sustain. 2 (2024) 27. https://doi.org/10.1038/s44296-024-00032-w.

[24] R.H. Bogue, The Chemistry of Portland Cement. Second Edition, Soil Science 79 (1955) 322.

[25] A. C33, ASTM C33 standard specifications for concrete aggregates, ASTM Standard Book (2003).

[26] B. EN, 12620, Granulats Pour Bétons Hydrauliques et Mortiers (2008).

[27] A. ASTM, Standard test method for relative density (specific gravity) and absorption of coarse aggregate, ASTM West Conshohocken, PA (2015).

[28] T. EN, 1097-6, 2013, Tests for Mechanical and Physical Properties of Aggregates-Part 6 (2013) 1–12.

[29] P. American Society for Testing and Materials, ASTM C136/C136M-19: Standard Test Method for Sieve Analysis of Fine and Coarse Aggregates, in: ASTM, 2019.

[30] B. En, Tests for Geometrical Properties of Aggregates-Part 1: Determination of Particle Size Distribution-Sieving Method, Czech Office for Standards, Metrology and Testing, Prague (2012) 933–1.

[31] P. ASTM, C29/C29M-17a. 2017, Standard Test Method for Bulk Density ("Unit Weight") and Voids in Aggregate (n.d.).

[32] B. EN, 1097-3: 1998, 1998. Tests for Mechanical and Physical Properties of Aggregates. Determination of Loose Bulk Density and Voids, British Standards Institution.

[33] H. Du, K.H. Tan, Properties of high-volume glass powder concrete, Cement and Concrete Composites 75 (2017) 22–29. https://doi.org/10.1016/j.cemconcomp.2016.10.010.

[34] M.S. Hassani, J.C. Matos, Y. Zhang, E.R. Teixeira, Green Concrete with Glass Powder—A Literature Review, Sustainability 15 (2023) 14864. https://doi.org/10.3390/su152014864.

[35] B. Sara, A. Mhamed, B. Otmane, E. Karim, Elaboration of a Self-Compacting mortar based on concrete demolition waste incorporating blast furnace slag, Construction and Building Materials 366 (2023) 130165. https://doi.org/10.1016/j.conbuildmat.2022.130165.

[36] B.C. Mendes, L.G. Pedroti, C.M.F. Vieira, J.M.F.D. Carvalho, J.C.L. Ribeiro, C.M.M.D. Souza, Application of mixture design of experiments to the development of alkali-activated composites based on chamotte and waste glass, Construction and Building Materials 379 (2023) 131139. https://doi.org/10.1016/j.conbuildmat.2023.131139.

[37] Stat-Ease, (n.d.). https://www.statease.com/ (accessed August 25, 2025).

[38] H. Singh, R. Siddique, Long term durability assessment of self-compacting concrete made with crushed recycled glass and metakaolin, Construction and Building Materials 400 (2023) 132656. https://doi.org/10.1016/j.conbuildmat.2023.132656.

[39] M.H. Kumar, N.R. Mohanta, S. Samantaray, N.M. Kumar, Combined effect of waste glass powder and recycled steel fibers on mechanical behavior of concrete, SN Appl. Sci. 3 (2021) 350. https://doi.org/10.1007/s42452-021-04353-6.

[40] M. Nili, H. Sasanipour, F. Aslani, The Effect of Fine and Coarse Recycled Aggregates on Fresh and Mechanical Properties of Self-Compacting Concrete, Materials 12 (2019) 1120. https://doi.org/10.3390/ma12071120.

[41] B. Sara, A. Mhamed, B. Otmane, E. Karim, Elaboration of a Self-Compacting mortar based on concrete demolition waste incorporating blast furnace slag, Construction and Building Materials 366 (2023) 130165. https://doi.org/10.1016/j.conbuildmat.2022.130165.

[42] S. Yehia, A. Douba, O. Abdullahi, S. Farrag, Mechanical and durability evaluation of fiber-reinforced self-compacting concrete, Construction and Building Materials 121 (2016) 120–133. https://doi.org/10.1016/j.conbuildmat.2016.05.127.

[43] A. Khaloo, E. Molaei Raisi, P. Hosseini, H. Tahsiri, Mechanical performance of self-compacting concrete reinforced with steel fibers, Construction and Building Materials 51 (2014) 179–186. https://doi.org/10.1016/j.conbuildmat.2013.10.054.

[44] T. Ahmad Wani, S. Ganesh, Study on fresh properties, mechanical properties and microstructure behavior of fiber reinforced self compacting concrete: A review, Materials Today: Proceedings 62 (2022) 6663–6670. https://doi.org/10.1016/j.matpr.2022.04.666.

[45] Bibm, et al., The European Guidelines for Self-Compacting Concrete: Specification, Production and Use, 563, Eur. Guidel. Self-Compact. Concr. 22, (n.d.). http://www.efnarc.org/pdf/SCCGuidelinesMay2005.pdf.

[46] P.A. Sivanantham, G.G. Prabhu, G.G. Vimal Arokiaraj, K. Sunil, Effect of Fibre Aspect-Ratio on the Fresh and Strength Properties of Steel Fibre Reinforced Self-Compacting Concrete, Advances in Materials Science and Engineering 2022 (2022) 1–8. https://doi.org/10.1155/2022/1207273.

[47] V. Corinaldesi, G. Moriconi, Mechanical and thermal evaluation of Ultra High Performance Fiber Reinforced Concretes for engineering applications, Construction and Building Materials 26 (2012) 289–294. https://doi.org/10.1016/j.conbuildmat.2011.06.023.

[48] R. Rachid, A. Mohamed, R. Mohamed, O. Mohammed, Effect of additions on the self-compacting concrete's absorption, J. Eng. Exact Sci. 9 (2023) 16058–01e. https://doi.org/10.18540/jcecvl9iss6pp16058-01e.